Anal. Chem. **2010,** *82,* 4145–4150

Electrokinetic Lab-on-a-BioChip for Multi-ligand/ Multi-analyte Biosensing

Ganeshram Krishnamoorthy,* Edwin T. Carlen, Hans L. deBoer, Albert van den Berg, and Richard B. M. Schasfoort

BIOS Lab-on-a-Chip Group, MESA+ Institute for Nanotechnology, University of Twente, P.O. Box 217, 7500 AE Enschede, The Netherlands

We present a simple electrokinetic lab-on-a-biochip (EKLB) with four microchannels integrated with a surface plasmon resonance imaging (iSPR) label-free biosensor that is operated using a single electrical voltage for the simultaneous transport of reagents in all microchannels without conventional fluidic plumbing. We demonstrate the utility of the simple approach with various biosensing experiments, including single injection kinetics (multiple varied ligand densities and single analyte concentration), one shot kinetics (single ligand densities and multiple varied analyte concentrations), and multi-ligand/multi-analyte detection. In all cases, the binding kinetics and affinity were extracted using a conventional 1:1 interaction model. Since the reagent transport is done with a single electrical voltage source, scaling up to hundreds to thousands of simultaneous experiments is straightforward.

Label-free biosensors are becoming commonly used to detect biological moieties in solution using a variety of detection techniques, such as, electrochemical, mechanical, or optical.[1] The simultaneous detection of multiple biomolecular targets, also known as a multiplex assays, such as nucleic acids, antibodies, and proteins, is important for medical diagnostics. For example, multiplex assays are important for the detection of respiratory pathogens because many different pathogens present similar symptoms; accurate pathogen identification and fingerprinting are important for patient recovery and public health monitoring.[2] Multiplex assays are also important for diagnosing cancers.[3,4] Multiplex label-free bioassays have been previously reported.[5−9] The main advantages of bioassay multiplexing are related to experimental time reduction and reduced cost, since assays are performed simultaneously.

Optical biosensors based on surface plasmon resonance (SPR) are currently the most commonly used systems for label-free bioassays. The extension of the single spot SPR to imaging surface plasmon resonance (iSPR) biosensors and the integration with lab-on-chip (LOC) and microarrays is an ideal platform for multiplex assays,[10,11] where each ligand spot in the microarray is used as an individual sensing area with a unique functionality. Multiplex iSPR assays have been reported for various application areas such as serum antibody screening,[12] lipid−protein interactions,[13] blocking assays,[14] DNA−protein interactions,[15] food screening,[16] and monitoring autoantibodies.[17] Lab-on-a-chip technology is an important accompaniment to multiplex iSPR assays and especially for multi-analyte assays. Most of the commercially available SPR systems, such as the Biacore[18] and Bio-Rad[19] instruments, are integrated with automatic computer controlled LOC systems and multiple syringe pumps for sample and reagent delivery. The number of flow cells is limited due to complex plumbing work required. Therefore, an alternate transport method that can reduce the complexity of the fluidic interconnects will aid in scaling the instruments to larger numbers of simultaneous measurements that can take advantage of conventional microarray ligand spot densities.

We recently demonstrated the integration of iSPR with electrokinetic (EK) focusing, electro-osmotic flow (EOF), and mi-

* To whom correspondence should be addressed. Phone: 0031 53 4892724. Fax: 0031 53 4893595. E-mail: g.krishnamoorthy@tnw.utwente.nl.

(1) Qavi, A. J.; Washburn, A. L.; Byeon, J.-Y.; Bailey, R. C. *Anal. Bioanal. Chem.* **2009**, *394*, 121–135.
(2) Hinman, A. R. *Vaccine* **1998**, *16*, 1116–1121.
(3) Wulfkuhle, J. D.; Liotta, L. A.; Petricoin, E. F. *Nat. Rev. Cancer* **2003**, *3*, 267–275.
(4) Zheng, G.; Patolsky, F.; Cui, Y.; Wang, W. U.; Lieber, C. M. *Nat. Biotechnol.* **2005**, *23*, 1294–1301.
(5) Yue, M.; Majumdar, A.; Thundat, T. In *BioMEMS and Biomedical Nanotechnology*, Vol. IV, Biomolecular Sensing, Processing and Analysis; Ferrari, M.; Bashir, R.; Wereley, S., Eds.; Springer Science + Business Media LLC: New York, 2006; pp 21−33.
(6) Brunker, S. E.; Cederquist, K. B.; Keating, C. D. *Nanomedicine* **2007**, *2*, 695–710.
(7) Zhao, Y.; Zhao, X.; Hu, J.; Xu, M.; Zhao, W.; Sun, L.; Zhu, C.; Xu, H.; Gu, Z. *Adv. Mater.* **2008**, *21*, 569–572.
(8) Szmacinski, H.; Ray, K.; Lakowicz, J. R. *Anal. Biochem.* **2009**, *385*, 358–364.
(9) Washburn, A. L.; Luchansky, M. S.; Bowman, A. L.; Bailey, R. C. *Anal. Chem.* **2010**, *82*, 69–72.
(10) Rothenhaeusler, B.; Knoll, W. *Nature* **1988**, *332*, 615–617.
(11) MacBeath, G.; Schreiber, S. L. *Science* **2000**, *289*, 1760–1763.
(12) Boer, A. R.; Hokke, C. H.; Deelder, A. M.; Wuhrer, M. *Glycoconjugate J.* **2008**, *25*, 75–84.
(13) Taylor, J. D.; Linman, M. J.; Wilkop, T.; Cheng, Q. *Anal. Chem.* **2009**, *81*, 1146–1153.
(14) Abdiche, Y. N.; Malashock, D. S.; Pinkerton, A.; Pons, J. *Anal. Biochem.* **2009**, *386*, 172–180.
(15) Boozer, C.; Ladd, J.; Chen, S.; Jiang, S. *Anal. Chem.* **2006**, *78*, 1515–1519.
(16) Raz, S. R.; Bremer, M. G. E. G.; Giesbers, M.; Norde, W. *Biosens. Bioelectron.* **2008**, *24*, 552–557.
(17) Lokate, A. M. C.; Beusink, B. J.; Besselink, G. A. J.; Pruijn, G. J. M.; Schasfoort, R. B. M. *J. Am. Chem. Soc.* **2007**, *129*, 14013–14018.
(18) Karlsson, R.; Kullman-Magnusson, M.; Hämäläinen, M. D.; Remaeus, A.; Andersson, K.; Borg, P.; Gyzander, E.; Deinum, J. *Anal. Biochem.* **2000**, *278*, 1–13.
(19) Bravman, T.; Bronner, V.; Lavie, K.; Notcovich, A.; Papalia, G. A.; Myszka, D. G. *Anal. Biochem.* **2006**, *358*, 281–288.

10.1021/ac1003163
Published on Web 04/19/2010

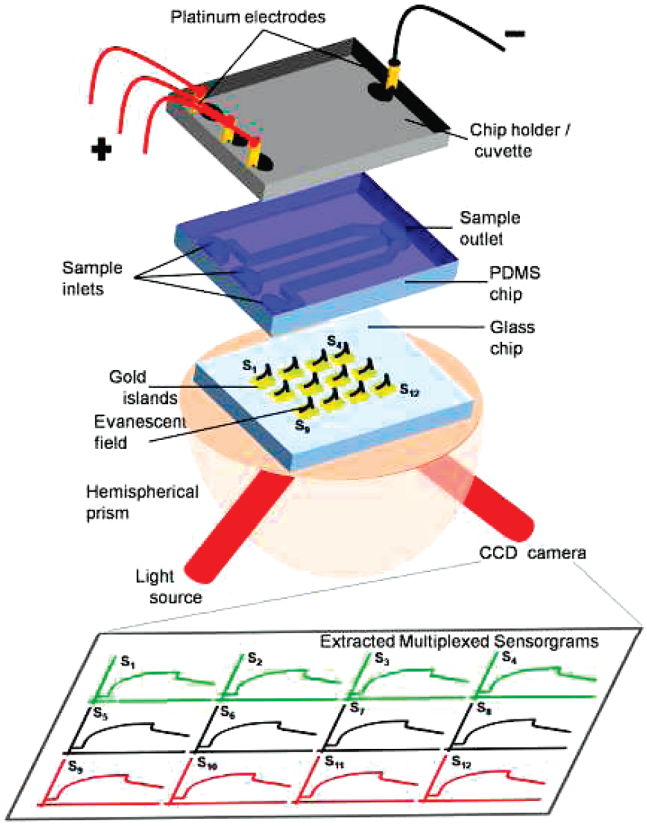

Figure 1. Illustration of the integrated surface plasmon resonance imaging system with our newly developed electrokinetic lab-on-a-biochip.

croarrays for multiplex bioassays.[20] However, sample cross contamination occurred at the gold sensing islands when the sample stream was focused to different locations. In addition, interchanging samples was complicated. In order to ameliorate the problems encountered with electrokinetic sample focusing, the chip was modified such that the single reaction chamber is divided into individual microchannels for each different ligand and/or analyte. This simplified approach leads to highly multiplexed multi-ligand/multi-analyte assays. A schematic illustration of the experimental setup is shown in Figure 1. The key advantages of the new configuration include pumpless and valveless EOF sample transport using a single dc voltage supply that is required for multiple channel simultaneous assay applications. The operational condition for using a single voltage supply is that the equivalent electrical resistance of the sample buffer in each microchannel should be approximately the same throughout the entire array to ensure the same flow rate in each channel.

Integrated microfluidics/SPR systems with multiple channels and pressure driven transport have been previously reported for applications including high-throughput screening[21−31] as well as small molecule detection.[32] These parallel device configurations can be used for multiple purposes, such as, the estimation of biomolecular interactions with a single injection of analytes[33] over various ligand densities, one-shot injection[19] of multiple analyte concentrations, and for multi-ligand/multi-analyte detection.[34] For the experiments presented here, we have considered three well-known interactant pairs: Fab fragments of human IgG−Fab specific antihuman IgG, β2microglobulin−antiβ2microglobulin, and neomycin−antineomycin. The kinetics and affinity of all interactant pairs were extracted from the measured iSPR sensorgrams. A detailed explanation of each different approach is described in the following sections. To the best of our knowledge, this is the first imaging system integrated directly with parallel flow channels using electrokinetic transport for biosensing applications.

MATERIALS AND METHODS

Microfabrication. The EKLB chip (size, 15 × 15 mm^2) consists of two layers. The 1.1 mm thick bottom glass layer, refractive index matched (n = 1.52) to the hemispherical prism of the iSPR instrument has an array of patterned 47 nm thick gold imaging islands (200 μm on a side) with 500 μm pitch for SPR imaging (SSens b.v. Hengelo, The Netherlands), shown in Figure 2a. The patterned gold imaging islands, called regions of interest (ROIs), were functionalized with a thiolated carboxymethyl dextran (CMD) layer for covalent ligand immobilization (XanTec GmbH, Germany). The top PDMS layer (2 mm thick) has the four microchannel structures, as well as reservoir holes (punched manually with a sharp hollow needle) for sample and electrode interfacing. The PDMS chips were ultrasonically cleaned in isopropanol for 15 min prior to any further processing and subsequently dried with dry nitrogen and cleaned with oxygen plasma for 5 min. Each reservoir hole is 2 mm in diameter and the depth of the microchannel is 40 μm. The four interaction channels are labeled as C_1, C_2, C_3, and C_4 each with width W_c = 220 μm and length L_c = 22 mm. The stamp and stick technique[35] was used to bond the PDMS chips to the glass chips with a thin layer of glue (optical adhesive 81, Norland) to one side of a microscope slide while continuously purged

(20) Krishnamoorthy, G.; Carlen, E. T.; Kohlheyer, D.; Schasfoort, R. B. M.; van den Berg, A. *Anal. Chem.* **2009**, *81*, 1957–1963.
(21) Piliarik, M.; Vaisocherová, H.; Homola, J. *Biosens. Bioelectron.* **2005**, *20*, 2104–2110.
(22) Homola, J.; Lu, H. B.; Nenninger, G. G.; Dostálek, J.; Yee, S. S. *Sens. Actuators, B* **2001**, *76*, 403–410.
(23) Berger, C. E. H.; Beumer, T. A. M.; Kooyman, R. P. H.; Greve, J. *Anal. Chem.* **1998**, *70*, 703–706.
(24) Dong, Y.; Wilkop, T.; Xu, D.; Wang, Z.; Cheng, Q. *Anal. Bioanal. Chem.* **2008**, *390*, 1575–1583.
(25) Lee, K.-H.; Su, Y.-D.; Chen, S.-J.; Tseng, F.-G.; Lee, G.-W. *Biosens. Bioelectron.* **2007**, *23*, 466–472.
(26) Situ, C.; Crooks, S. R. H.; Baxter, A. G.; Ferguson, J.; Elliott, C. T. *Anal. Chim. Acta* **2002**, *473*, 143–149.
(27) Naimushin, A. N.; Soelberg, S. D.; Nguyen, D. K.; Dunlap, L.; Bartholomew, D.; Elkind, J.; Melendez, J.; Furlong, C. E. *Biosens. Bioelectron.* **2002**, *17*, 573–584.
(28) Taylor, A. D.; Ladd, J.; Yu, Q.; Chen, S.; Homola, J.; Jiang, S. *Biosens. Bioelectron.* **2006**, *22*, 752–758.
(29) Wang, Z.; Wilkop, T.; Xu, D.; Dong, Y.; Ma, G.; Cheng, Q. *Anal. Bioanal. Chem.* **2007**, *389*, 819–825.
(30) Homola, J.; Dostálek, J.; Chen, S.; Rasooly, A.; Jiang, S.; Yee, S. S. *Int. J. Food Microbiol.* **2002**, *75*, 61–69.
(31) Palumbo, M.; Pearson, C.; Nagel, J.; Petty, M. C. *Sens. Actuators, B* **2003**, *90*, 264–270.
(32) Kawazumi, H.; Gobi, V. K.; Ogino, K.; Maeda, H.; Miura, N. *Sens. Actuators, B* **2005**, *108*, 791–796.
(33) Krishnamoorthy, G.; Carlen, E. T.; Beusink, B. J.; Schasfoort, R. B. M.; van den Berg, A. *Anal. Methods* **2009**, *1*, 162–169.
(34) Andersson, O.; Nikkinen, H.; Kanmert, D.; Enander, K. *Biosens. Bioelectron.* **2009**, *24*, 2458–2464.
(35) Schlautmann, S.; Besselink, G. A. J.; Radhakrishna Prabhu, G.; Schasfoort, R. B. M. *Micromech. Microeng.* **2003**, *13*, S81–S84.

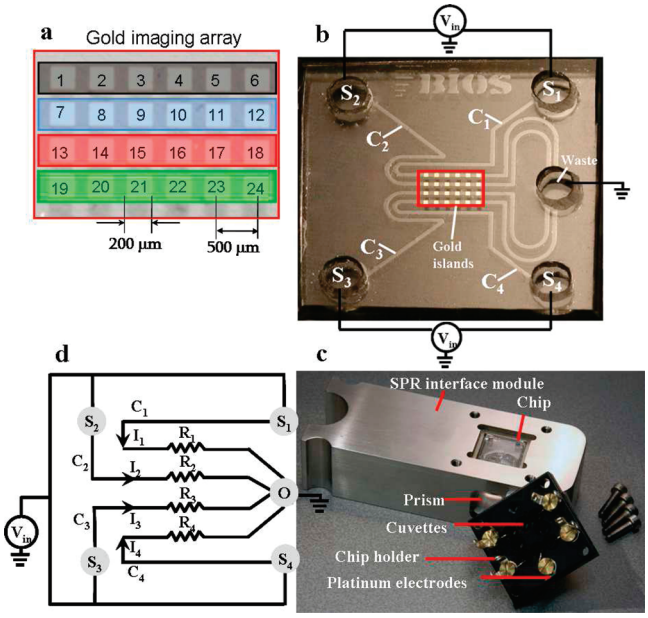

Figure 2. (a) 6 × 4 microarray of gold iSPR sensing islands and (b) 15 × 15 mm² glass−PDMS microfluidic chip showing channels C_1−C_4. S_1−S_4 are sample fluidic inlets. (c) iSPR interface module with chip fixture with integrated platinum electrodes. (d) Electrical circuit representation of the EKLB chip. R_1−R_4 represents electrical resistances in the respective channels. I_1−I_4 represents the electrical current in the respective channels. O represents the common fluidic outlet and electrical ground.

with dry nitrogen.[36] The molded PDMS layers were carefully pressed onto the glue blotter layer, removed, and subsequently bonded to the glass chip. The bonded stack was UV (359 nm) cured for 2 min. The final chip is shown in Figure 2b. The microchannel surfaces are hydrophilic following the plasma treatment, and all the channels were filled with HEPES buffer by capillary action prior to each experiment.

Surface Plasmon Resonance Imaging. The angle scanning iSPR system (IBIS-iSPR, IBIS Technologies b.v., Hengelo, The Netherlands) used for experiments has been described previously.[17,20,37] A refractive index change at the solution/gold interface is related to the amount of adsorption or binding of biomolecules at the surface, which results in a measurable shift of the SPR-dip. The measured SPR-dip position is translated into a time domain sensorgram, which contains the SPR angle shift (millidegrees, mdeg) on the ordinate and measurement time on the abcissca. The SPR angle shift is used as a response unit (RU) to quantify the binding of biomolecules to the sensing surface. A calibration indicated a RU = 1 mdeg corresponds to ~11 pg/mm² of protein on the sensing surface. There are three main measurement phases of the sensorgram: (1) baseline phase, a running buffer in contact with the sensor surface to establish the baseline responses; (2) association phase, sample containing the target analyte [A] is injected to the interaction chamber and the ligands [B] immobilized on the surface, the capturing element on the sensor surface binds to the target resulting in complex formation [AB]; and (3) dissociation phase, injection of a running buffer again which leads to dissociation of bound

(36) Jeong, H. E.; Suh, K. Y. *Lab Chip* **2008**, *8*, 1787–1792.
(37) Beusink, J. B.; Lokate, A. M. C.; Besselink, G. A. J.; Pruijn, G. J. M.; Schasfoort, R. B. M. *Biosens. Bioelectron.* **2008**, *23*, 839–844.

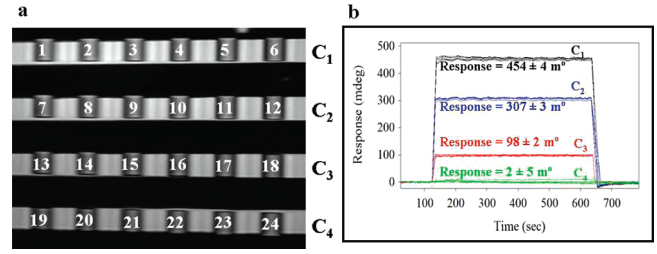

Figure 3. (a) iSPR image of the chip with gold sensing islands. (b) Measured iSPR response for different glycerol concentrations showing the largest response for the highest concentration (C_1) and lowest response for the lowest concentration C_4).

molecules from the surface. The microfabricated chip was placed on the hemispherical prism (with a droplet of refractive index matching oil) that is integrated into the SPR interface module (Figure 2c).

RESULTS AND DISCUSSION

Multiple experiments were conducted with the new EKLB chip. Prior to experiments, two-dimensional finite element simulations were performed to estimate the electrokinetic sample flow rate with respect to applied voltage across the channel and buffer conductivity (see the Supporting Information). Electrokinetic flow profiles were imaged using fluorescence microscopy (see the Supporting Information) and real-time iSPR imaging with a glycerol calibration sample. Finally, biomolecular interaction experiments were performed. Details about the performed experiments are discussed in the respective discussion sections below.

iSPR Flow Profiling. The SPR responses and real-time images were recorded with injections of various concentrations (0, 1, 2, and 3%) of glycerol in 10 mM HEPES buffer. The real time iSPR image of the EKLB chip is shown in Figure 3a. The resulting iSPR sensorgrams are shown in Figure 3b. The total measurement time is 800 s in which 120 s of baseline measurement with 10 mM HEPES buffer followed by 500 s of glycerol injection (V_{in} = 200 V dc) and 180 s of 10 mM HEPES buffer again. In C_1, a 3% glycerol solution resulted in measured response of 454 ± 4 mdeg. In C_2, a 2% glycerol solution resulted in measured response of 307 ± 3 mdeg. In C_3, a 1% glycerol solution resulted in measured response of 98 ± 4 mdeg. In C_4, the signal observed was 2 ± 5 mdeg.

Biomolecular Interaction Measurements. Multiple types of biomolecules (the immobilized biomolecules are ligands and the biomolecules in flow are analytes) have been used in the experiments: ligand 1, Fab of Human IgG (Sigma, The Netherlands); ligand 2, neomycin (Sigma, The Netherlands); ligand 3, β2microglobulin (Sigma, The Netherlands); analyte 1, Fab specific goat antihuman IgG (Jackson ImmunoResearch Laboratories, Inc.); analyte 2, antineomycin (Biodesign International); analyte 3, mAb for β2microglobulin (Abcam, Inc.). All the samples were injected with a constant voltage V_{in} = 200 V dc (IBIS Technologies b.v., Hengelo, The Netherlands). Prior to the biomolecular interaction experiments, the chip with gold sensing array coated with CMD was activated with 0.4 M EDC and 0.1 M NHS for 20 min followed by rinsing with acetic acid to maintain the pH suitable for immobilization. The chip was completely dried with nitrogen. After the immobilization of biomolecules, the active sites were blocked with 1 M ethanolamine followed

Table 1. Scenario 1 Results[a]

channels	interactant pairs	response (t = 500 s) mdeg	k_a ($\times 10^4$) M^{-1} s^{-1}	k_d ($\times 10^{-4}$) s^{-1}	R_{max} mdeg	K_D nM
C_1		28 ± 3	5.8 ± 2.1	1.3 ± 2.1	34 ± 3.0	2.2 ± 1.1
C_2	H IgG Fab− Fab specific AH IgG	17 ± 1	6.7 ± 3.6	0.9 ± 0.1	22 ± 1.5	1.3 ± 0.8
C_3		11 ± 1	7.6 ± 1.8	0.8 ± 0.3	15 ± 1.2	1.3 ± 1.0
C_4	buffer					

[a] Various concentrations of human IgG Fabs immobilized and single concentration of Fab specific antihuman IgG as the analyte (n = 6).

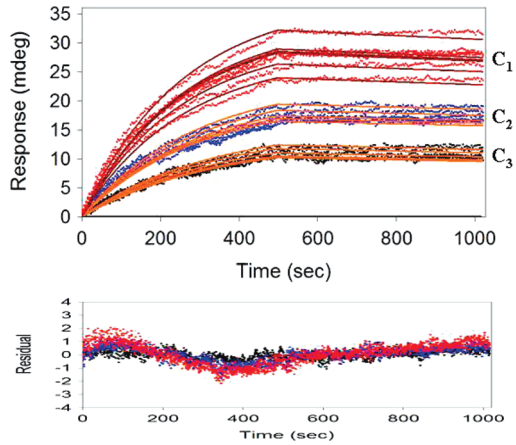

Figure 4. Experiment and model fit (orange curves) results of scenario 1: (a) The concentrations of human IgG Fabs immobilized are C_1 = 2 mg/mL, C_2 = 1 mg/mL, C_3 = 0.5 mg/mL, and C_4 = 0 mg/mL. The analyte concentrations in all the channels are 50 nM. The residuals of the model fit are shown in the lower plot.

by washing with 10 mM HEPES buffer. Various experiments performed include scenario 1, single injection kinetics;[33] four different concentrations of ligand 1 (C_1 = 2 mg/mL, C_2 = 1 mg/mL, C_3 = 0.5 mg/mL, and C_4 = 0 mg/mL) in 50 mM MES buffer (pH 5.4) were immobilized and single concentration of analyte 1 ($C_1 = C_2 = C_3 = C_4$ = 50 nM) was injected into the chip using EOF (V_{in} = 200 V dc). This also gives information about reproducibility of the extracted kinetics with respect to various densities of ligand immobilized on the surface, which might provide information about rebinding effects, steric hindrance, and mass transport limitations. Scenario 2, one shot kinetics;[19] a single concentration of ligand 1 ($C_1 = C_2 = C_3 = C_4$ = 2 mg/mL) was immobilized, and a different concentration of analyte 1 (C_1 = 12.5 nM, C_2 = 25 nM, C_3 = 50 nM, and C_4 = 0 nM) was injected into the chip. As described in the literature,[19] this approach reduces the duration of kinetics experiments where various concentrations of analytes used for kinetics and affinity parameter extraction could be done with a single injection of various concentrations of analytes in different channels simultaneously. Scenario 3, multi-ligand/multi-analyte detection;[34] three different ligands (C_1 = 85 mg/mL ligand 3, C_2 = 20 mg/mL ligand 2, and C_3 = 2 mg/mL ligand 1) were immobilized each in one channel and three different analytes (C_1 = 35 nM analyte 1, C_2 = 110 nM analyte 2, and C_3 = 50 nM analyte 3), which is specific to these ligands, are injected into the respective channels. In all the cases, after immobilization, the remaining active sites were blocked with 1 M ethanolamine (Sigma, The Netherlands) for 10 min and subsequently washed prior to biomolecular interaction experiments. A baseline measurement was performed using a 10 mM HEPES buffer for 100 s. In all experiments, the association phase was measured for 500 s followed by a dissociation phase with a running buffer for 500 s. The measured sensorgrams were fitted to a 1:1 interaction model[38] using the commercially available software (Scrubber, Biologics Inc., Australia). The results are discussed below in detail.

Scenario 1: Single Injection Kinetics. The first biomolecular interaction experiment performed with the EKLB chip was a single injection kinetics measurement. The immobilization of different concentrations of ligand 1 were performed using the electrokinetic voltage V_{in}=100 V dc for 30 min. The biomolecular interaction was carried out with analyte 1. The resultant sensorgram is shown in Figure 4 together with the 1:1 model function. The residuals of the fit are shown in the bottom plot. Results are shown in different colors. The extracted parameters are shown in Table 1. The affinity constant calculated in three channels varies between 1.3 and 2.2 nM. Channel 1, which has the highest concentration of immobilized ligand shows larger response variations. The standard errors shown in the table are calculated from the six ROIs that are in a single channel. The large variations could be due to the fact that the ligand was not uniformly immobilized in the channel. The model fit is in good agreement for the lower concentration ligands. The deviation from the model fit was observed for the higher ligand concentration measurements and is due to the fact that molecules are completely saturated or active sites are not accessible by the analyte molecules. High analyte concentrations can also lead to mass transport limited interactions.[39−41] Analyte concentrations for the kinetics experiment have to be in the range of the affinity constants to estimate the accurate results. In this experiment, we have included high analyte concentrations and used the conventional 1:1 interaction model fit for the demonstration purpose only. In channel 1, the topmost sensorgram is far away from the rest of the sensorgrams. This is most likely due to fabrication problem with the gold sensing array. The standard error is comparatively less in the scenario 2 experiments.

Scenario 2: One Shot Kinetics. The second demonstration that we have performed with the EKLB chip is one shot kinetics as previously reported.[19] The immobilization of ligand 1 followed by blocking and washing steps were done prior to the bonding of the top layer of the chip. In this way, the electrical contact time with the surface gets reduced because of the offline immobilization. The interaction was performed with various concentrations

(38) Morton, T. A.; Myszka, D. G.; Chaiken, I. M. *Anal. Biochem.* **1995**, *227*, 176–185.
(39) Schuck, P. *Biophys. J.* **1996**, *70*, 1230–1249.
(40) Myszka, D. G.; Morton, T. A.; Doyle, M. L.; Chaiken, I. M. *Biophys. Chem.* **1997**, *64*, 127–137.
(41) Glaser, R. W. *Anal. Biochem.* **1993**, *213*, 152–161.

Table 2. Scenario 2 Results[a]

channels	interactant pairs	response (t = 500 s) mdeg	k_a ($\times 10^4$) M^{-1} s^{-1}	k_d ($\times 10^{-5}$) s^{-1}	R_{max} mdeg	K_D nM
C_1	HIgG Fabs−Fab specific AHIgG	35 ± 2	5.2 ± 2.2	9.7 ± 4.9	37 ± 3.2	1.9 ± 0.7
C_2		24 ± 1				
C_3		16 ± 2				
C_4	buffer					

[a] Single concentration of human IgG Fabs immobilized and various concentrations of Fab specific antihuman IgG as the analyte (one concentration in each channel; n = 6).

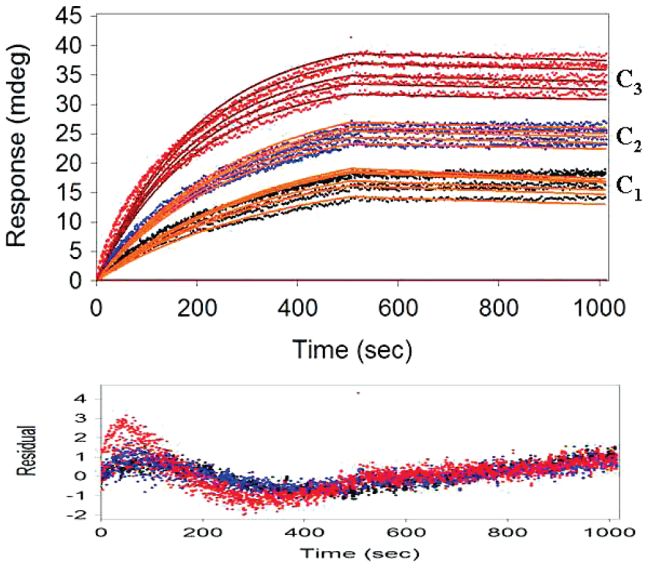

Figure 5. Experiment and model fit (orange curves) results of scenario 2: (a) The concentrations of human IgG fabs immobilized in all the channels are 2 mg/mL. The analyte concentrations used are C_1 = 12.5 nM, C_2 = 25 nM, C_3 = 50 nM, and C_4 = 0 nM as reference. The residuals of the model fit are shown in the lower plot.

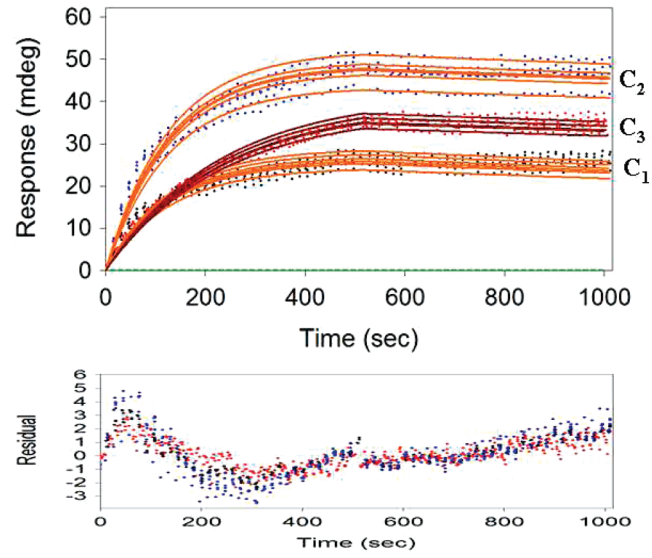

Figure 6. Experiment and model fit (orange curves) results of scenario 3: (a) C_1 = 85 μg/mL β2microglobulin immobilized and 35 nM antiβ2microglobulin as the analyte; C_2 = 20 mg/mL neomycin immobilized and 110 nM antineomycin as the analyte; C_3 = 2 mg/mL human IgG Fabs immobilized and 50 nM antihuman IgG specific to Fab as analyte; C_4 = 10 mM HEPES as a reference. The residuals of the model fit are shown in the lower plot.

of analyte 1. The resultant sensorgram and its 1:1 model fit are shown in Figure 5. The residual plots are shown in the lower plot in Figure 5. This is an ideal experiment that also works in the classical kinetics approach where various concentrations of analytes were used for the extraction of kinetics and affinity parameters of the interactant pairs. The experimental data and fit are in good agreement in this case. Higher analyte concentrations used in channel 3 slightly deviate from the 1:1 interaction model, which is reproducible when we compare the results of the experiment in scenario 1. The response level observed was in the same range, and the standard error is slightly lower in this case.

The association rate (k_a), as well as, dissociation rate (k_d) extracted using a global fit analysis are quite similar to the values extracted in scenario 1 and are shown in Table 2. The large distribution observed in k_a and k_d is due to the deviations observed in responses. Proper immobilization or well quantified immobilization would be helpful in order to reduce the response variations.

Scenario 3: Multi-ligand/Multi-analyte Detection. When kinetics information of a biomolecular interaction is not important, especially in the case of biodetections or diagnostics, a single analyte (normally serum) is injected to detect and identify the presence of specific proteins or antibodies in the samples. If multiple components have to be detected in parallel, the assay time could be reduced which can make diagnostics faster. To demonstrate this scenario, we used each of the single channels for single interactant pairs and hence detected three different interactant pairs at the same time. The fourth channel is used for referencing with the 10 mM HEPES buffer.

In this experiment, we see three different resultant sensorgram profiles as well as 1:1 model fits shown in Figure 6. The extracted parameters for all three interactant pairs are listed in Table 3. In this case, similar results were observed in the case of human IgG Fabs that were used in the previous experiments. The responses and extracted parameters are in the same range. We have chosen three well-known interactant pairs for this experiment to demonstrate the concept of the new chip. All three interactant pairs follow the conventional 1:1 interaction model when the proper analyte and ligand concentration is used for the experiments. For quantitative detection purposes, kinetics information is very important and can be extracted straightaway from the recorded sensorgram. Our chip is useful for multi-ligand/multi-analyte detection, but also for the simultaneous measurement of binding kinetics information of multiple interactant pairs.

There are some areas for future development in order to take full advantage of this method. The chips have been used for prototype development, and this general technique can be transferred to other materials such as glass. Another area for future development is overcoming the problem of gold degrada-

Table 3. Scenario 3 Results[a]

channels	interactant pairs	response (t = 500 s) mdeg	k_a ($\times 10^4$) M^{-1} s^{-1}	k_d ($\times 10^{-4}$) s^{-1}	R_{max} mdeg	K_D nM
C_1	neomycin−antineomycin	47 ± 3	7.4 ± 3.6	1.7 ± 1.1	50 ± 3.0	2.3 ± 0.9
C_2	HIgG Fabs−Fab Specific AHIgG	35 ± 1	8.5 ± 2.8	1.1 ± 0.8	41 ± 1.4	1.3 ± 0.8
C_3	β2microglobulin-antiβ2microglobulin	26 ± 2	22 ± 12	1.9 ± 1.0	27 ± 1.7	0.9 ± 0.5
C_4	buffer					

[a] Various ligands immobilized in each channel and various analyte antibodies specific to the immobilized ligands (n = 6).

tion. We have observed that low conductivity buffers resulted in reduced damage to the gold sensing regions following a series of experiments. Hydrolysis appears to lead to bubble formation in such circumstances on the corners of the gold sensing array, which then leads to the detachment of the gold from the surface. This might be due to oxidation and subsequent removal of the titanium adhesion layer. Other adhesion layers, such as tantalum, can avoid this problem (results not shown). Coating of the gold layers with a functionalized hydrogel layer reduced the degradation of the gold layer.[33]

CONCLUSIONS

We have demonstrated various examples of biosensing scenarios including multi-ligand/multi-analyte detection with the new integrated label-free iSPR system with electrokinetic sample transport. The demonstration of the multi-ligand/multi-analyte concept using electrokinetic transport shows a new direction for integrated biosensing chips when large numbers of reagents are simultaneously processed and measured. At present, the chip design can be extended to more than 10 individual microchannels (dimensions are currently limited to the imaging area of the CCD camera of the iSPR system), where each channel has 12 sensing locations, which results in a measurement matrix of more than 100 sensing regions that can be measured simultaneously.

SUPPORTING INFORMATION AVAILABLE

Additional information as noted in text. This material is available free of charge via the Internet at http://pubs.acs.org.

Received for review February 4, 2010. Accepted April 5, 2010.

AC1003163